Avrupa Bilim ve Teknoloji Dergisi
Özel Sayı 32, S. 14-19, Aralık 2021

Araştırma Makalesi

www.ejosat.com ISSN:2148-2683

European Journal of Science and Technology
Special Issue 32, pp. 14-19, December 2021

Research Article

A Study on the Effects of the Interior Architecture on the Fracture Toughness of 3D Printed PLA Samples

Cem Boğa[1*], Mirsadegh Seyedzavvar[2]

[1*]Adana Alparslan Türkeş Science and Technology University, Faculty of Engineering, Department of Mechanical Engineering, Adana, Turkey,(ORCID: 0000-0002-9467-1141), cboga@atu.edu.tr
[2]Adana AlparslanTürkeş Science and Technology University, Faculty of Engineering, Department of Mechanical Engineering, Adana, Turkey, (ORCID: 0000-0002-3324-7689), mseyedzavvar@atu.edu.tr

(International Conference on Design, Research and Development (RDCONF) 2021 – 15-18 December 2021)

(**DOI:** 10.31590/ejosat.1039951)

ATIF/REFERENCE: Boğa, C. & Seyedzavvar, M. (2021). A Study on the Effects of the Interior Architecture on the Fracture Toughness of 3D Printed PLA Samples. *European Journal of Science and Technology*, (32), 14-19.

Abstract

Additive manufacturing (AM) using 3D printing techniques is widely used not only in prototyping, but also in production of structural elements in many applications such as medical science and biomechanical engineering. Therefore, it is highly important to investigate the fracture mechanics of components and engineering materials made with 3D printing techniques with the aim of application in biomechanical components. In this study, to investigate the effects of interior architecture on the mixed mode fracture behavior of 3D printed polylactic acid (PLA) components, special Arcan samples were produced at 70% filling ratio and four different filling types using fused filament fabrication technique. A special fixture has been designed that allowed the mixed-mode fracture experiments of the Arcan samples to be conducted on a unidirectional tensile test machine. The fracture tests were performed under 3 different loading angles of 0°, 45° and 90° as opening mode, mixed mode I / II and shear mode, respectively. In addition, the finite element analyses were also conducted to determine the geometric functions of the Arcan samples required for calculation of fracture toughness at different loading angles. Overall, the results of fracture toughness tests revealed that for the sections of the samples that are mainly exposed to opening and mixed-mode loading conditions, printing with the triangular filling pattern provides higher fracture toughness to the final products. In contrast, for the sections exposed to pure shear loadings, hexagonal printing pattern provides a better resistance against fracture.

Keywords: Additive manufacturing, 3D printing, PLA, Arcan samples, Mixed-mode fracture.

İç Mimarinin 3D Baskılı PLA Numunelerinin Kırılma Tokluğuna Etkileri Üzerine Bir Araştırma

Öz

3D baskı tekniklerini kullanan eklemeli üretim (EÜ), yalnızca prototiplemede değil, tıp bilimi ve biyomekanik mühendisliği gibi birçok uygulamada yapısal elemanların üretiminde de yaygın olarak kullanılmaktadır. Bu nedenle biyomekanik bileşenlerde uygulamak amacı ile 3D baskı teknikleri ile yapılmış bileşenlerin ve mühendislik malzemelerinin kırılma mekaniğinin araştırılması oldukça önemlidir. Bu çalışmada, iç mimarinin 3D baskılı polilaktik asit (PLA) bileşenlerinin karışık mod kırılma davranışı üzerindeki etkilerini araştırmak için, erimiş filament fabrikasyon tekniği kullanılarak %70 doluluk oranı ve dört farklı dolgu tipinde özel Arcan numuneleri üretilmiştir. Arcan numunelerinin karışık modlu kırılma deneylerinin tek yönlü bir çekme test makinesinde gerçekleştirilmesine izin veren özel bir fikstür tasarlanmıştır. Kırılma testleri sırasıyla 0°, 45° ve 90° olmak üzere 3 farklı yükleme açısı altında açılma modu, karışık mod I/II ve kayma modu olarak gerçekleştirilmiştir. Ayrıca, farklı yükleme açılarında kırılma tokluğunun hesaplanması için gerekli olan Arcan numunelerinin geometrik fonksiyonlarını belirlemek için sonlu elemanlar analizleri de yapılmıştır. Genel olarak, kırılma tokluğu testlerinin sonuçları, numunelerin çoğunlukla açılma ve karışık mod yükleme koşullarına maruz kalan bölümleri için üçgen dolgu deseni ile baskı yapılmasının nihai ürünlere daha yüksek kırılma tokluğu sağladığını ortaya koymuştur. Buna karşılık, saf kayma yüklemelerine maruz kalan kesitler için altıgen baskı deseni kırılmaya karşı daha iyi bir direnç sağlamıştır.

Anahtar Kelimeler: Eklemeli imalat, 3D baskı, PLA, Arcan örnekleri, Karışık mod kırılması.

[*]Corresponding Author: cboga@atu.edu.tr

1. Introduction

Polylactic acid (PLA), a renewable aliphatic polyester, is a widely used material and in terms of the volume of production, ranks first among bioplastics in the world (Nagarajan et al., 2016). PLA is one of the most widely used filament materials for the production of prostheses in 3-dimensional (3D) printers, especially in medical applications. Fused filament fabrication process (FFF), an additive manufacturing method, is used as one of the main techniques in the production of PLA samples due to the ease and flexibility in prototyping parts. Nowadays, the use of 3D printed components in biomedical applications has increased significantly. Therefore, researchers are putting intense efforts to produce 3D printed components with reliable strength and high mechanical properties. More specifically, there have been studies in the literature on both the mechanical properties of industrial materials and their fracture behavior under mixed-mode loadings.

Singh et al. (2020) employed 3D printing technology to evaluate the mechanical properties of chitosan reinforced PLA specimens. Experiments were conducted to investigate the effects of chitosan additive, filler density and annealing temperature on the mechanical behavior of PLA composite specimens. They determined that the chitosan reinforcement and the filling density were important parameters in the strength of composite specimens, but the annealing temperature did not affect it much.

Torun et al. (2020) produced zigzag printed PLA samples to examine the effects of filling ratios on the mixed-mode fracture behavior of 3D printer components. For all filling ratios, they reported that when the loading angle was increased from 0° to 90°, the shear mode stress intensity factor increased and the tension (opening) mode critical stress intensity factor decreased.

Sedighi et al. (2020) produced polycarbonate samples with the FFF method in order to investigate the effect of layer orientation on tensile, bending and fracture behavior. First, they determined the mode-I fracture toughness values for different build directions in the samples. Overall, the results of tensile, bending and fracture experiments of the polycarbonate samples revealed the anisotropy properties of the 3D printed components.

Kaya et al. (2020) investigated the fracture behavior of different crack geometries at different temperatures and deformation rates in S-2 glass/epoxy composite samples by both experimental and finite element methods. They reported the dependency of the fracture behavior of composite samples to the temperature and the loading conditions.

Fonseca et al. (2019) produced samples by 3D printing from pure and short carbon fiber reinforced Polyamide 12 (PA 12) material. They determined pure mode-I laminar fracture toughness with the produced double cantilever beam (DCB) samples. They stated that the material toughness of the samples increased significantly in carbon fiber reinforced samples.

Cantrell et al. (2017) produced 3D printed acrylonitrile butadiene styrene (ABS) samples with various raster and build orientation. They carried out experiments to determine the mechanical properties of the produced samples. They showed that the parameters such as raster and build orientations have negligible effects on the modulus of elasticity and Poisson's ratio of the samples.

Gardan et al. (2016, 2019) examined the cracking response of 3D-printed compact-tensile specimen made of thermoplastic filaments and studied the mode-I fracture behavior of CT specimens made of ABS.

The literature review revealed the existing gap in the thorough knowledge that is necessary to characterize the fracture and crack growth behavior of materials such as PLA processed by FFF technique and employed as structural elements in many applications such as medical science and biomechanical engineering (dentistry, orthopedics, bio-implants, etc.). There are also many unknown issues regarding the effects of FFF process parameters on the fracture toughness of the 3D printed components. Therefore, the lack of a comprehensive research on the mixed-mode fracture behavior of these newly developed structural parts has been the main motivation for our study. It is therefore essential to use an appropriate test specimen and procedure to determine the fracture behavior of such materials. It is also important to characterize how the processing of 3D printed materials in different interior architectures will affect their load carrying capacity. Therefore, in this study, the mixed-mode fracture behavior of samples produced with 70% pristine PLA polymer at four different interior architectures in FFF process was investigated by performing a series of fracture experiments to fill the research gaps in this area. The results of experiments, combined with a FEA developed for specially designed Arcan samples, were employed to determine the fracture toughness of 3D printed PLA samples with different internal architectures.

2. Material and Method

Fracture and tensile samples were produced on a Flashforge Creator-3 FFF machine, equipped with a dual extruder, using 1.75 mm diameter white PLA filament and filling ratio of 70% and 0.12 mm of layer thickness. The nozzle and table temperatures were set as 210 and 80 °C respectively. The printing speed and travel speed were selected as 50 and 70 mm/sec, respectively. In order to determine the mechanical properties of 3D printed structures, the dogbone samples were printed according to ASTM D638-14. The printing process of Arcan fracture and tensile test samples are represented in Figure 1.

Figure 1. An overview of 3D printing process of tensile and Arcan fracture samples.

The uniaxial tensile tests were performed using a Shimadzu AGS-X 100 kN tensile testing machine (Figure 2). All tests were performed at room temperature and constant loading rate of 1 mm/min. Also, the extension and transverse contraction of the tensile test samples were recoded using a camera extensometer and the acquired data have been later processed to determine the Poisson's ratio of the printed samples.

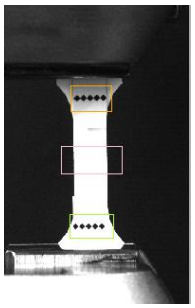

Figure 2. A representation of a dogbone sample on a Shimadzu AGS-X 100 kN tensile testing machine

The calculated mechanical properties of 3D-printed PLA samples for different filling types after the tensile test are given in Table 1.

According to the Table 1, the highest tensile strength values belong to the sample with the triangle filling type (Boğa et al., 2021). As shown in Figure 3, specially designed single-edge notched Arcan specimens and an in-house developed mixed-mode loading fixture were used to perform mode-I, mode-II and I/II mixed-mode fracture toughness tests.

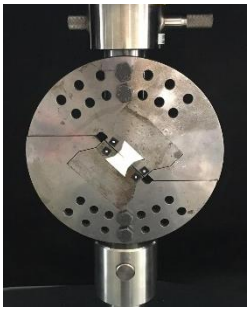

Figure 3. A representation of fracture test setup for testing an Arcan sample under loading angle of 45°.

Fracture test specimens have been mounted on the fixture to create a mixed-mode stress field at the crack tip of such specimens. Under these conditions, crack propagation is related to the stress intensity factor at the crack-tip. The stress field at the crack-tip of the single-edge notch specimen is schematically shown in Figure 4.

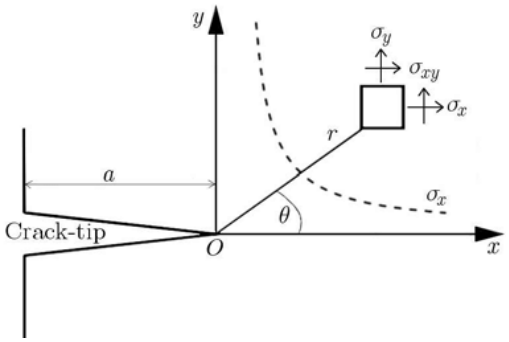

Figure 4. Crack-tip stress field under mixed-mode loading (Moustabchir et al., 2015).

Stress areas at the crack-tip can be expressed in terms of the normal and shear stresses as in Eq. (1).

Table 1. Mechanical properties of PLA samples with different internal architectures (Boğa et al., 2021).

Materials	***Yield Stress (MPa)***	***Ultimate Stress (MPa)***	***Modulus of Elasticity (GPa)***	***Poisson's Ratio***
Line	14.0	15.64	2.3	0.213
Hexagon	14.7	15.05	2.41	0.124
Triangle	19.5	22.76	2.63	0.355
3D Infill	15.3	17.15	2.0	0.342

$$\sigma_{xx} = \frac{K_I}{\sqrt{2\pi r}}\cos\frac{\theta}{2}\left[1-\sin\frac{\theta}{2}\sin\frac{3\theta}{2}\right] - \frac{K_{II}}{\sqrt{2\pi r}}\sin\frac{\theta}{2}\left[2+\cos\frac{\theta}{2}\cos\frac{3\theta}{2}\right]$$
$$\sigma_{yy} = \frac{K_I}{\sqrt{2\pi r}}\cos\frac{\theta}{2}\left[1+\sin\frac{\theta}{2}\sin\frac{3\theta}{2}\right] + \frac{K_{II}}{\sqrt{2\pi r}}\sin\frac{\theta}{2}\cos\frac{\theta}{2}\cos\frac{3\theta}{2} \quad (1)$$
$$\tau_{xy} = \frac{K_I}{\sqrt{2\pi r}}\cos\frac{\theta}{2}\sin\frac{\theta}{2}\cos\frac{3\theta}{2} + \frac{K_{II}}{\sqrt{2\pi r}}\cos\frac{\theta}{2}\left[1-\sin\frac{\theta}{2}\sin\frac{3\theta}{2}\right]$$

Here, K_I and K_{II} are the stress intensity factors at the crack-tip for mode-I and mode-II loadings, respectively. The strain energy release rate for mixed mode loading could be expressed as in Eq. (2);

$$G_T = G_I + G_{II} = \frac{K_I^2}{E'} + \frac{K_{II}^2}{E'} \quad (2)$$

where G is the energy release rate for crack propagation, E is the modulus of elasticity of the sample, and v is the Poisson's ratio. $E' = E$ is valid for plane stress and $E' = E/(1-\nu^2)$ is applied

in plane strain conditions. Furthermore, as shown in Figure 5, numerical modeling of crack under mixed loading conditions using the ABAQUS/CAE finite element program was used to determine and analyze the strain field distribution and geometry shape function of fracture samples near the notch crack-tip.

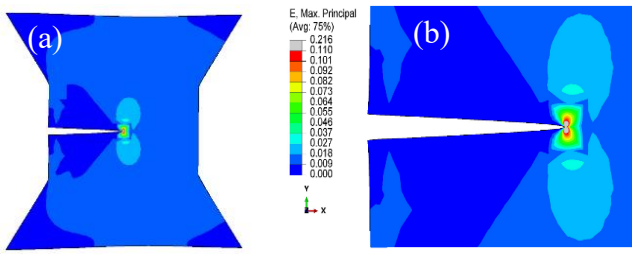

Figure 5. An overview of distribution of maximum principal stain under typical mode-I loading of Arcan sample; a) Arcan specimen and b) focused view of crack-tip.

Eqs. 3 and 4 were used to obtain the critical stress intensity factor values (K_I and K_{II}) of the printed samples.

$$K_I = \frac{P_C}{wt}\sqrt{\pi a} f_I(a/w) \quad (3)$$

$$K_{II} = \frac{P_C}{wt}\sqrt{\pi a} f_{II}(a/w) \quad (4)$$

where *f(a/w)* is geometrical factor, P_C is the fracture load, *a* is the crack length, *t* is the specimen thickness and *w* is the specimen width.

3. Results and discussion

In this section, the results of fracture tests are presented. As explained before, experiments were carried out to investigate the effects of interior architecture on the fracture behavior of PLA samples made by FFF technique. The tests were repeated at least three times for each infill type and loading angle, and the average load-displacement curves were reported as the result of fracture test under specific experimental set. The load-displacement plots obtained with the tensile testing machine were used to determine the maximum loads and displacement at fracture. The results of force-displacement curves for Arcan samples of different interior architectures under fracture loading of 0°, 45° and 90° are presented in Figure 6(a) to (c), respectively. As shown in Figures. 6(a) and (b), the triangular structure represented the highest fracture load either at opening or mixed-mode fracture loadings. In contrast, according to Figure (c), the samples with hexagonal internal architecture showed the highest shear strength. The linear structure represented the highest crack-mouth opening before fracture. However, the lowest fracture resistance belongs to the samples of 3D infill filling pattern.

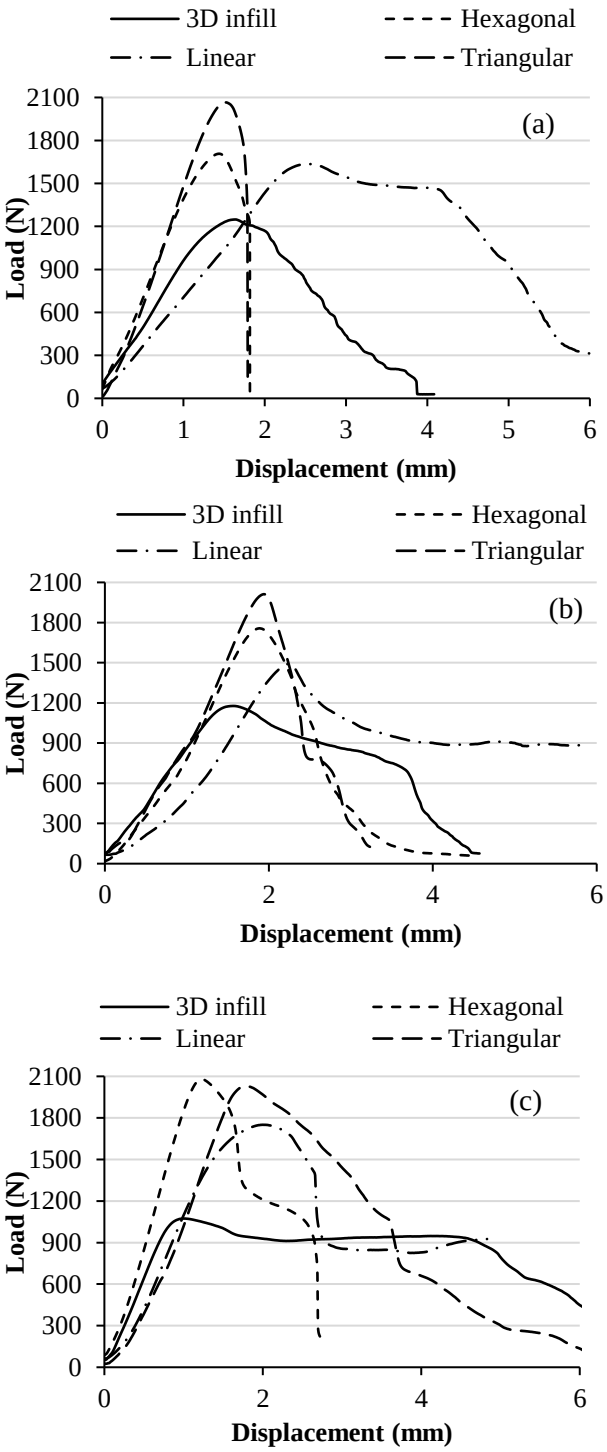

Figure 6. Load versus displacement diagrams of pristine PLA 3D printed Arcan specimen under; (a) opening (0°), (b) I/II mixed (45°) and (c) shear (90°) mode of loading.

Each material breaks at a certain critical stress value. The stress density measured at this critical stress value at which the material breaks gives the fracture toughness value of that material. This fracture toughness value is also a property of that material. The

unit of this material property, also known as the stress intensity factor, is found as $MPa\sqrt{m}$ and is denoted by K_{IC} (Uğuz, 1996). The critical stress intensity factors determined experimentally under 0°, 45° and 90° loading conditions are presented collectively in Table 2. As can be seen in this table, the samples of triangular and 3D infill filling types represented the highest and lowest fracture toughness values under opening mode of loading with the K_{IC} = 2.03 and 1.14 [$MPa.m^{1/2}$], respectively. This pattern for the shear mode of loading was observed for the samples with hexagonal and 3D infill internal architectures with the K_{IIC} = 1.65 and 0.84 [$MPa.m^{1/2}$], respectively. Overall, the results of fracture toughness tests revealed that for the sections of the samples that are mainly exposed to opening and mixed mode loading conditions, printing with the triangular filling pattern provides the highest fracture toughness of the final product. In contrast, for the sections exposed to pure shear loadings, hexagonal printing pattern provides a better resistance against fracture.

Table 2. K_C ($MPa\sqrt{m}$) values for different filling types

Filling types	Critical stress intensity factor	0°	45°	90°
3D Infill	K_{IC}	1.14	0.78	0
	K_{IIC}	0	1.07	0.84
Line	K_{IC}	1.61	0.99	0
	K_{IIC}	0	1.36	1.32
Triangle	K_{IC}	2.03	1.33	0
	K_{IIC}	0	1.83	1.61
Hexagon	K_{IC}	1.59	1.17	0
	K_{IIC}	0	1.61	1.65

Table 3. Average critical strain energy release rates $(G)_C$ [J/m^2] for different filling types

Filling types	Critical strain energy release rates	0°	45°	90°
3D Infill	$(G_I)_C$	573.797	268.620	0
	$(G_{II})_C$	0	505.494	311.535
	$(G_T)_C$	573.797	774.114	311.535
Line	$(G_I)_C$	1075.869	406.797	0
	$(G_{II})_C$	0	767.689	723.195
	$(G_T)_C$	1075.869	1174.486	723.195
Triangle	$(G_I)_C$	1369.416	587.823	0
	$(G_{II})_C$	0	1112.872	861.381
	$(G_T)_C$	1369.416	1700.695	861.381
Hexagon	$(G_I)_C$	1032.875	559.275	0
	$(G_{II})_C$	0	1059.022	1112.298
	$(G_T)_C$	1032.875	1618.297	1112.298

The critical strain energy release rates (G_C) calculated for different interior architectures of the FFF samples are shown in Table 3. These quantities indicate how much energy must be given to create new fracture surfaces at the crack-tip of the samples. The $(G_I)_C$, $(G_{II})_C$ and the resultant of $(G_T)_C$ values based on the experimental values obtained for different interior architecture of 3D printed samples and using Eq. 2 are given in Table 3. As can be seen in Table 3, the samples of triangular filling type represented the highest strain energy release rate with value of ~1369 J/m^2 under opening mode of loading. $(G_I)_C$ appears to be greater than $(G_{II})_C$ for all filling types, showing that the propagation of crack in mode-I loading requires higher energy as compared to mode-II loading.

In this study, the mixed-mode fracture behavior of samples produced with 70% pristine PLA polymer at four different interior architectures in FFF process was investigated by performing a series of fracture experiments. The results of experiments, combined with a FEA developed for specially designed Arcan samples, were employed to determine the fracture toughness of 3D printed PLA samples with different internal architectures. The outstanding results of this research are as follows:

1. Among the 3D printed samples with different internal architectures, the ones with triangular structure represented the highest fracture load either at opening or mixed-mode fracture loadings. In contrast, the samples with hexagonal internal architecture showed the highest shear strength. The linear structure represented the highest crack-mouth opening before fracture. However, the lowest fracture resistance belongs to the samples of 3D infill filling pattern.
2. The samples of triangular and 3D infill filling types represented the highest and lowest fracture toughness values under opening mode of loading with the K_{IC} = 2.03 and 1.14 [$MPa.m^{1/2}$], respectively. This pattern for the shear mode of loading was observed for the samples

4. Conclusions

with hexagonal and 3D infill internal architectures with the K_{IIC} = 1.65 and 0.84 [$MPa.m^{1/2}$], respectively.

3. The samples of triangular filling type represented the highest strain energy release rate with the value of ~1369 J/m^2 under opening mode of loading. $(G_I)_C$ appears to be greater than $(G_{II})_C$ for all filling types, showing that the propagation of crack in mode-I loading requires higher energy as compared to mode-II loading.
4. The results of fracture toughness tests revealed that for the sections of the samples that are mainly exposed to opening and mixed mode loading conditions, printing with the triangular filling pattern provides the highest fracture toughness of the final product. In contrast, for the sections exposed to pure shear loadings, hexagonal printing pattern provides a better resistance against fracture.

5. Acknowledge

This work was supported by Adana Alparslan Türkeş Science and Technology University Scientific Research Coordination Unit. Project Number: 20103002.

References

Nagarajan, V., Mohanty, A. K., & Misra M. (2016). Perspective on polylactic acid (PLA) based sustainable materials for durable applications: Focus on toughness and heat resistance. *ACS Sustainable Chemistry & Engineering*, 4(6), 2899-2916. https://doi.org/10.1021/acssuschemeng.6b00321

Singh, S., Singh, G., Prakash, C., Ramakrishna, S., Lamberti, L., & Pruncu, C. I. (2020). 3D printed biodegradable composites: An insight into mechanical properties of PLA/chitosan scaffold. *Polymer Testing*, 89, Article 106722. https://doi.org/10.1016/j.polymertesting.2020.106722

Torun, A. R., Yıldız, E. C., Kaya, Ş. H., & Choupani, N. (2020). Mixed-mode fracture behavior of 3D-printed PLA with zigzag filling. *Green Materials*, 9(1), 1-8. https://doi.org/10.1680/jgrma.20.00013

Sedighi, I., Ayatollahi, M., Bahrami, B., Martínez, M. P., & Garcia-Granada A. A. (2020). Mechanical behavior of an additively manufactured poly-carbonate specimen: tensile, flexural and mode I fracture properties. *Rapid Prototyping Journal*, 26(2), 267–277. https://doi.org/10.1108/RPJ-03-2019-0055

Kaya, Z., Balcıoğlu, H. E., & Gün, H. (2020). The effects of temperature and deformation rate on fracture behavior of S-2 glass/epoxy laminated composites. *Polymer Composites*, 41(11), 1–12. https://doi.org/10.1002/pc.25753

Fonseca, J., Ferreira, I. A., Moura, M. F. D., Machado, M., & Alves, J. L. (2019). Study of the interlaminar fracture under mode I loading on FFF printed parts. *Composite Structures*, 214, 316-324. https://doi.org/10.1016/j.compstruct.2019.02.005

Cantrell, J., Rohde, S., Damiani, D., Gurnani, R., DiSandro, L., Anton, J., Young, A., Jerez, A., Steinbach, D., Kroese, C., & Ifju, P. (2017). Experimental characterization of the mechanical properties of 3D-printed ABS and polycarbonate parts. *Rapid Prototyping Journal*, 23(4), 811-824. https://doi.org/10.1108/RPJ-03-2016-0042

Gardan, J., Makke, A., & Recho, N. (2016). A method to improve the fracture toughness using 3D printing by extrusion deposition. *Procedia Structural Integrity*, 2, 144-151. https://doi.org/10.1016/j.prostr.2016.06.019

Gardan, J., Makke, A., & Recho, N. (2019). Fracture Improvement by Reinforcing the Structure of Acrylonitrile Butadiene Styrene Parts Manufactured by Fused Deposition Modeling. *3D Printing and Additive Manufacturing*, 6(2), 113-117. https://doi.org/10.1089/3dp.2017.0039

Boğa, C., Seyedzavvar, M., & Zehir, B. (2021). Experimental Investigation on the Effects of Internal Architecture on the Mechanical Properties of 3D Printed PLA Components. *European Journal of Science and Technology*, 24, 119-124. https://doi.org/10.31590/ejosat.901012

Moustabchir, H., Arbaoui, J., Zitouni, A., Hariri, S., & Dmytrakh, I. (2015). Numerical analysis of stress intensity factor and t-stress in pipeline of steel P264GH sumbitted to loading conditions. *Journal of Theoretical and Applied Mechanics*, 53(3), 665─672. https://doi.org/10.15632/jtam-pl.53.3.665

Uğuz, A. (1996). *Kırılma Mekaniğine Giriş*. Uludağ Üniversitesi Basımevi, Bursa, pp 123.